Displacement Wave Accumulation of the Floating Bridge Subjected to Speedy and Heavy Load

JIANG Zhao-bing[1,2], LIU Hua[1], CHEN Yun-he[2] , CHEN Xu-jun[2]

(1. School of Naval Architecture, Ocean & Civil Engineering, Shanghai Jiao Tong University, Shanghai 200240, China;
2. Engineering Institute of Engineering Corps, PLA University of Science & Technology, Nanjing 210007, China)

Abstract—The stiffness and the propagation velocity of displacement wave of a long floating bridge are much less than those of regular steel or concrete bridge. The effect of the displacement wave accumulation will occur at the floating bridge subjected to fast and heavy moving load when the velocity of the load is faster than that of the propagation of displacement wave. The dynamic equation of the floating bridge is introduced briefly and solved employing the finite element method. The wave phenomenon will be existed at the floating bridge motion and the wave accumulation effect will be occurred when the velocity of the load is much speedy. The wave accumulation effect is appeared at the corresponding model experiment and the result validates the theory and the numerical simulation of the dynamics of the floating bridge. The numerical and the model test both indicate that the wave accumulation effect is more obvious when the load is heavier and the velocity of the load is faster. The load with high-speed will come forth the phenomenon of velocity vibration because of the existing of the wave accumulation. The displacement wave accumulation effect and the vibration of loading velocity will be existed at the civil distributing supporting and flexible super-long bridges (such as the suspension bridge and the cable-stayed bridge) subjected to speedy and heavy loads. So there is significant academic value and widely technical application to study and solve this new wave model.

Index Terms—Floating bridge; Speedy and heavy load; Effect of wave accumulation; Velocity vibration; Model test

1 INTRODUCTION

Temoshinko S. [1] studied the resonance of the first vibration shape of a simply-supported-beam bridge caused by a fast velocity moving load. He found that the bridge is resonated when the whole time for a moving load to pass the bridge is equivalent to half of the period of the first vibration shape. The maximum dynamic displacement of the bridge is 50% larger than the static one when the bridge is resonant. And when the load just passes the bridge, maximum displacement of the bridge occurs. Y. Sato and S. Okamoto et al[2] studied the accumulation of ground surface wave under high-velocity train. By experiment, they found that the accumulation of the ground surface wave would be taken place when the train velocity approaches the wave propagation velocity in the ground. Then they analyzed the accumulation displacement by means of a certain theory. Bian Xue-cheng[3] developed a hybrid method of 2.5 dimensional finite element and layer element to study dynamic ground response due to moving loads. The time histories of ground responses and wave motion are presented, and it is found that significant wave propagations are generated when Mach number of moving load approaches or exceeds 1.0. High-level vibrations identified to be similar to supersonic booms in fluid dynamics have been observed when train run with speed close to or exceeding the surface wave velocities in the surrounding ground. In 2001, Torbjörn Ekevin, Martin X.D.Li et al[4] studied the dynamic responses of the Winkler-beam under moving loads with different velocities. And then they developed effective numerical procedures of adaptive finite element method for solving problems associated with wave propagation in the track-ground system. Result indicates that the response for train velocities below the critical wave velocity for the structure is more or less quasistatic. However, as the speed increases and exceeds the critical wave velocity, the response of the railroad structure and the ground material changes dramatically. Waves are created from the origin of the load and propagate in the ground material[5]. In 2006, Torbjörn Ekevin and Håkan Lane et al[6] deal with quality controlled FE-procedures for wave propagation including error estimation and mesh refinement/coarsening. The numerical result shows that when a high-speed train approaches an area with decreasing thickness of underlying soft soil on a stiff rock it is expected that the reflection of the wave will increase the total amplitude of the wave. And when the slope of the ground was introduced, wave magnitudes were clearly greater behind the train. Y. B. Yang, H. H. Hung, et al [7] studied the transmissibility of soils for vibrations induced by trains moving at different speeds employing the 2.5D finite/infinite element approach. And two train speeds are considered, i.e. 70m/s and 100m/s, to stand for the sub-critical and super-critical ranges. With different factors including the shear speed, damping ratio, stratum depth, etc, the results all show when the train speed is larger than the Rayleigh wave speed of the layered soils the wave phenomena are more evident and the amplitudes of the ground wave are larger than the one with speed lower than the Rayleigh wave speed.

Chen and Ju et al[8]have pointed out that conducting an analysis of wave propagation in soil/rock is fundamental in predicting the possible vibration level. Kouroussis and Verlinden et al[9] have investigated the generation and propagation of ground vibrations induced by railway traffic, more specifically in the case of urban vehicles. Chen and Lin et al[10] have examined two simple analysis models for wave propagation in order to evaluate their reliability in measuring ground vibrations induced by high-speed trains. Yang and Hung, et al[11] have introduced a new method to the out-of-plane wave transmission. And this 2.5D approach can capture the three-dimensional wave propagation effect using a two-dimensional finite/infinite element mesh. Hughes and Reali et al[12] have

studied the discretezation behavior of classical finite element and NURBS approximations on problems of structural vibrations and wave propagation. Erkan and Seyhan et al[13] have investigated the wave propagating characteristics and frequency-dependent screening effects of the wave barriers according to various isolation material stiffness.

All the above-mentioned wave phenomena are created when the velocity of the loads subjected to the structures is high. The wave accumulations are presented when the velocity of the moving load is higher than (or equivalent to) the one of the structure wave propagation. These accumulations will induce to the increasing of reflections and forces acted on the structures, and will increase the force acted on the load and decrease the velocity of the loads passing by. Moreover, the flexibilities of the distribute-supported flexible long bridges (including the long floating bridge, large-span suspension bridge and cable-stayed bridge, etc.) are larger, and the wave phenomena will be more evident and be trend to the effect of wave accumulations.

The following argument and analysis of the numerical calculation and experiment of the wave accumulation effect are presented for the floating bridge subjected to fast and heavy moving load. This paper is organized as follows: In Section 2 we firstly describe the dynamic equations of floating bridge subjected to moving load. In Section 3 we report the dynamic responses of floating bridge, including static case and dynamic cases under speedy and heavy load. In Section 4 we report the model experiment results, compare the calculating results with the experimental data and demonstrate what the displacement wave accumulation is. In Section 5 we discuss the results of the displacement wave accumulation of the floating bridge subjected to speedy and heavy load, and predict that the displacement wave accumulation will be occurred on the suspension bridge or the cable-stayed bridge subjected to high-speed and heavy load.

2 DISCRIPTION OF THE DYNAMIC EQUATION

The motion equations governing the dynamic response of the floating bridge can be derived by assuming the work of external forces to be absorbed by the work of internal, inertial and viscous forces, for any small kinetically admissible motion[14]. On the basis of the FEM and local separation of variables, the equilibrium equations of the floating bridge can be expressed as:

$$[M]\{\ddot{D}\}+[C]\{\dot{D}\}+[K]\{D\}=\{R^{ext}\}, \tag{1}$$

where $\{\ddot{D}\}$, $\{\dot{D}\}$ and $\{D\}$ are respectively the acceleration, velocity and displacement vectors of floating bridge; $[M]$, $[C]$ and $[K]$ are respectively the mass, damping and stiffness matrices of the floating bridge; $\{R^{ext}\}$ is the external load vectors. Floating bridge external load $\{R^{ext}\}$ consists of the body force $\{R_1^{ext}\}$, and surface force $\{R_2^{ext}\}$ and the concentrated force $\{R_3^{ext}\}$, and is variable with time. The stiffness matrix $[K]$ can be assembled by the standard FEM procedures to overlap the element stiffness matrix $[k]$.

As for a floating bridge with uniform mass distribution, the body force (the weight of the floating bridge) can be balanced by the static buoyancy (the integration of static pressure over undisturbed wetted surface); therefore, only the unbalanced force originating from the dynamic and the moving distributive force count.

The oscillating body in the fluid will cause the movement of surrounding water; inversely, the inertial forces of water will induce the reactive forces to the wetted surface of the body, which can be written as:

$$\{R_2^{ext}\}_1=\sum_{S_w}\int_{S_{we}}[N]^T\{\Phi\}\mathrm{d}S_{we}, \tag{2}$$

where S_{we} is the element area of the wetted surface and S_w is the total area of the wetted surface; $[N]$ is the shape function, and $\{\Phi\}$ is the prescribed surface traction force and has the form as:

$$\{\Phi\}=-\frac{M_{ea}}{S_{we}}\{\ddot{a}\}, \tag{3}$$

where M_{ea} is the element added mass of the wetted surface obtained by Todd's method[15]; $\{\ddot{a}\}$ is the acceleration vector for any point in the wetted element and can be known from the nodal acceleration vector $\{\ddot{d}\}$,

$$\{\ddot{a}\}=[N]\{\ddot{d}\}. \tag{4}$$

Substituting Eqs.(3) and (4) into Eq.(2) and assuming t_{we} to be the uniform thickness of the wetted element will produce:

$$\{R_2^{ext}\}_1=-[M_a]\{\ddot{D}\} \tag{5}$$

with

$$[M_a]=\sum_{S_{we}}[m_{ea}], \tag{6}$$

$$[M_{ca}]=\int_{V_{we}}[N]^T\frac{M_{ea}}{S_{we}t_{we}}[N]\mathrm{d}V_{we}, \tag{7}$$

where $V_{we}=S_{we}t_{we}$ is the volume of the wetted element; and $\{\ddot{D}\}$ is constructed by standard FEM procedures, i.e. conceptual expansion of element matrices to "structure size".

Based on the classification of the mass matrix, Eq.(7) can be termed the consistent added matrix. The diagonal matrix form of the added mass matrix is computed by evenly assigning M_{ea} to the translational DOFs of the node in each wetted element; however, structural added mass matrix $[M_a]$ must be calculated by standard FEM procedures with non-zero on the corresponding DOFs between the interfaces and the fluid and zeros on the remaining.

The so-called hydrostatic force is defined as wetted surface distributed force produced by the buoyancy when the floating bridge is away from the equilibrium position. Assuming the force is linear with the vertical displacement of the floating bridge and uniformly acts upon the structural wetted surface, the

$$\{R_2^{ext}\}_2=\sum_{S_w}\int_{S_{we}}-[N]^T\frac{p_b}{S_{we}}\{u\}\mathrm{d}S_{we}, \tag{8}$$

where p_b is the hydrostatic pressure of unit displacement and can be determined from the draft-displacement curve; and $\{u\}$ is the displacement of any point in the wetted element and can be obtained from the nodal displacement vector $\{d\}$,

$$\{u\}=[N]\{d\}. \tag{9}$$

Then similar to Eq.(5), we have

$$\{R_2^{ext}\}_2=-[K_b]\{D\} \tag{10}$$

with

$$[K_b]=\sum [k_b], \tag{11}$$

$$[k_b]=\int_{V_{we}} [N]^T \frac{p_b}{S_{we}t_{we}}[N]\mathrm{d}V_{we}. \tag{12}$$

The expression of $[k_b]$ in Eq.(12) has the same form as Eq.(7) and is specified as the consistent form of the hydrostatic force. Similarly, the distributed element force is evenly assigned to the wetted surface nodes to form the element diagonal hydrostatic force matrix, and $[K_b]$ is the hydrostatic force coefficients matrix with non-zeros on the element nodal DOFs of the wetted surface and zeros on the remaining.

On the assumption that the vehicles are always in contact with the surface of the floating bridge leaving out of consideration of elastic and damping features, we will have the surface distributed load due to the gravitation and the inertial force of the motion. Here, the gravitation load of the vehicles is:

$$\{R_2^{ext}\}_2 = \sum_{E_{vall}} \delta(\mathrm{num}(E_{ve})-\mathrm{num}(E_{vt})) \int_{E_{ve}} [N]^T \{p_v\}(t)\mathrm{d}S_{ve}, \tag{13}$$

where, E_{vall} and E_{vt} respectively represent all the loaded elements in the procedure of motion and the elements subjected to the moving load at time t ; and E_{ve} is one of the element E_{vt}; num( ) denotes the element number; δ is the Dirac function; S_{ve} indicates the area of E_{ve}; $\{p_v(t)\}=P_v/A(t)$ implies the gravity distribution density of all loaded elements at time t, with P_v being the weight of the load and $A(t)$ the loaded area at time t.

The structural inertial force due to the moving load can be given by

$$\{R_2^{ext}\}_4 = -\sum_{E_{vall}} \delta(\mathrm{num}(E_{ve})-\mathrm{num}(E_{vt})) \int_{E_{ve}} [N]^T \rho_v(t)[N]\{\ddot{d}\}\mathrm{d}S_{ve} \tag{14}$$

where $\rho_v(t)=p_v(t)/g$ is the surface density of mass distribution on all loaded elements. Provided that all the above elements have the uniform thickness t_{ve}, Eq.(14) becomes:

$$\{R_2^{ext}\}_4=-[M_v(t)]\{\ddot{D}\} \tag{15}$$

with

$$[M_v(t)] = \sum_{E_{vall}} \delta(\mathrm{num}(E_{ve})-\mathrm{num}(E_{vt}))[m_v], \tag{16}$$

$$[m_v]= \int_{V_{ve}} [N]^T \frac{\rho_v(t)}{S_{ve}t_{ve}}[N]\mathrm{d}V_{ve}, \tag{17}$$

where $V_{ve}=S_{ve}t_{ve}$ is the volume of the loaded elements; $[M_v(t)]$ is the moving mass matrix due to the inertial forces of the load with non-zeros on the DOFs of the loaded elements at time t and zeros on the remaining.

Various kinds of linear and nonlinear damping are usually simplified as the viscous damping in structural dynamic problems, which is convenient to be dealt with numerically. A popular spectral damping scheme, called Rayleigh or proportional damping[15] is often used to form the damping matrix as a linear combination of the stiffness and mass matrices of the structure, that is:

$$[C]=\alpha[K]+\beta[M], \tag{18}$$

where α and β are called the stiffness and mass proportional damping constants, respectively, which can be associated with the fraction of critical damping ξ by

$$\xi=0.5\left(\alpha\omega+\frac{\beta}{\omega}\right). \tag{19}$$

Therefore, α and β can be determined by choosing the fractions of critical damping (ξ_1 and ξ_2) at two different frequencies (ω_1 and ω_2):

$$\begin{cases}\alpha=2(\xi_2\omega_2-\xi_1\omega_1)/(\omega_2^2-\omega_1^2)\\ \beta=2\omega_1\omega_2(\xi_1\omega_2-\xi_2\omega_1)/(\omega_2^2-\omega_1^2)\end{cases}. \tag{20}$$

Substituting Eqs.(5) , (10) and (15) into Eq.(1), one can derive the governing equation of the floating bridge subjected to a moving load, and the equation is as follows:

$$[M]+[M_a]\{\ddot{D}\}+[C]\{\dot{D}\}+[K]\{D\}=\{P_v(t)\}-[M_v(t)]\{\ddot{D}\}-\{R_{con}^{\mathrm{int}}\} \tag{21}$$

where $\{P_v(t)\}=\{R_2^{ext}\}_3$.

3 Numerical Simulations

3.1 static case

Considering the floating bridge composed of 15 pontoon bridges and the length of each one is L=6.7m, the width is B=8.082m, the depth is D=1.07m, the weight of the load is $P_v(t)$ = 230.3kN . Fu[16] discretized the floating bridge by the combination of the shell and elements and we calculate the static response of the floating bridge no considering the nonlinear of the gaps between pontoon bridges employing the average stiffness method. And the comparison of our present calculation, Fu's result and the experimental data[16] is as Fig.1.

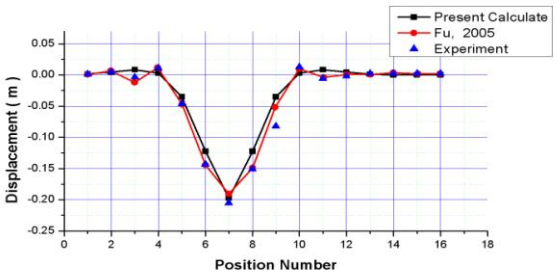

Fig.1 Comparison of responses of the floating bridge at static state

3.2 dynamic cases

When the velocity of a moving load is low, the deflection of the floating bridge only takes place at limited range and the displacement curve can be treated as left-and-right symetry about the acting point of the load. Fig. 2 demonstrates the temporal displacement variation of the floating bridge when the velocity of load is v=1.0m/s .

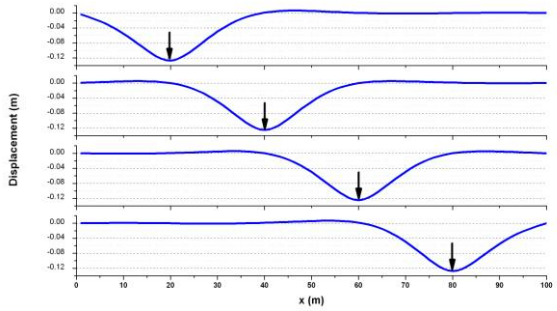

Fig. 2 Temporal displacement variation of floating bridge subjected to moving load (v=1.0m/s)

But when the moving load has high-velocity, the load will excite displacement wave of the floating bridge and the wave will propagate along the floating bridge from load point to two ends. Moreover, the displacement curve is not symmetry, for the velocity has direction and the displacement curve is obviously asysmmetry for the floating bridge subjected to faster moving load, as Fig. 3 shows.

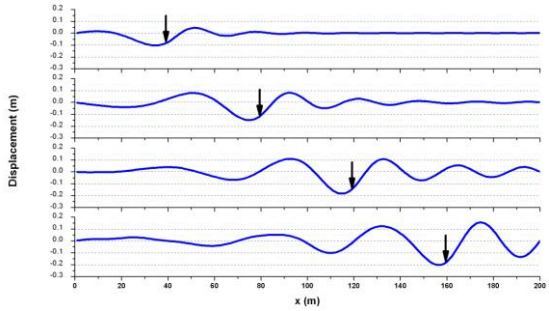

Fig.3 Temporal displacement variation of floating bridge subjected to moving load (v=50.0m/s)

Comparing the displacement of floating bridge subjected to low velocity load with the one to high velocity load, the moving load with high velocity, which is equivalent to the velocity of displacement wave, will chase after the wave and make the displacement wave accumulate in front of the load point. Then larger displacement will be generated and the amplitude of displacement wave may equivalent to the maximum displacement. This phenomenon is obviously showed at Fig.3.

Fig.3 also demonstrates that the wave length transmitting ahead is smaller that the one transmitting backwards. By calculation, the wave length of displacement wave ahead is about 50.0m/s and the one backwards is about 70.0m/s . This phenomenon means that the displacement wave accumulation will be obvious when the velocity of moving load is equivalent to the velocity of the displacement wave. And the moving load will be the state of climbing slope, which will enlarge the resistant force acting on the load and make the load velocity low. Results from academic analysis will be verified by the latter model experiment.

The phenomena of displacement wave accumulation and climbing slope of moving load will also be verified by the temporal displacement curve of the midpoint of floating bridge. The curve in Fig. 4 is the temporal displacement curve of the midpoint of floating bridge under moving loads with velocities 1.0m/s and 50.0m/s , respectively. Fig. 4 shows that the floating bridge is not warped airwards of when the load velocity is equal to 1.0m/s and the moving load is approach to midpoint. But the warped displacement of the midpoint is about 0.05m when the velocity of the load is equal to 50.0m/s (or vt/L=0.43). Moreover, when the velocity of moving load is 50.0m/s , the maximum displacement of the midpoint for floating bridge is not taken place at non-dimensional time vt/L=0.5 but at vt/L=0.53. The displacement of the load point is smaller then the maximun one and the moving load is climbing slope all the time passing the floating bridge.

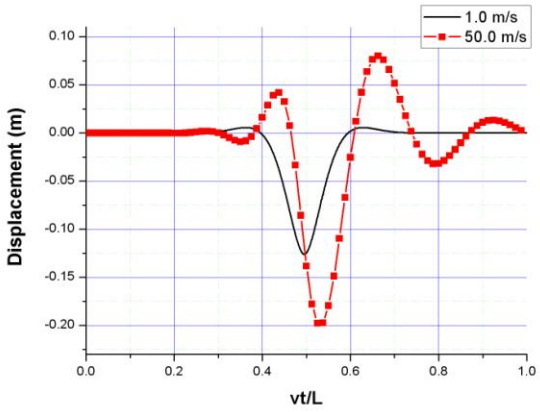

Fig. 4 Temporal displacement variation of the midpoint of floating bridge subjected to moving load

4 MODEL EXPERIMENT FOR THE DISPACEMENT WAVE ACCUMULATION OF FLOATING BRIDGE AND VELOCITY VIBRATION OF THE MOVING HEAVY LOAD

4.1 facture of the experimental model

The floating bridge is made of foam plates and the size of a single foam plate is 180.0cm×30.0cm×2.5cm. Totally, there are 14 foam plates forming the floating bridge and the translucent adhesive tape is used to conglutinate the foam plates together, so the total length of the floating bridge is 180.0cm×14=2520.0cm , and Fig.5 is the picture of the experimental model of floating bridge. We can measure the stiffness of the foam plates and the gaps between of them. For static or dynamic calculations of the floating bridge subjected to load, we give the foam plate and the gap with translucent adhesive tape with different stiffness of FEM element.

Fig. 5 Picture for the experimental model of floating bridge

The load model is made up of four-wheel trailer with some weights. Load case 1, case 2 and case 3 are made up of a big weight and trailer, three small weights and trailer and five small weights and trailer, respectively.

The trailer is tracted by electro-machine with shift gears and the velocities are controlled by the actiyator, as Fig.6. The maximum rotate speed of the electro-machine is 1500 turns per minute.

Fig. 6 Electro-machine and actiyator

The displacement of floating bridge is measured by mobile co-ordinate measurement machine, as Fig. 7. The measure resolution of the machine is 0.002mm and it is enough for displacement measure of floating bridge. The mobile co-ordinate measurement machine is mainly made up of three parts, including optical inductor, light-emitting diodes and data collection system. There are nine measure points disposed at the experiment, and the serial numbers of measure points at Fig. 8 are 1~9 from left to right. The detailed arrange is at [17].

Fig. 7 Mobile co-ordinate measurement machine

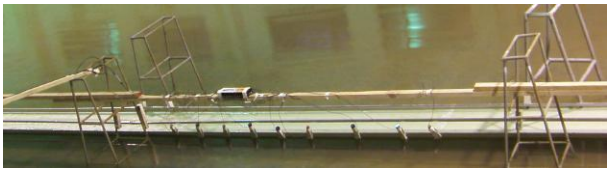

(a) Closed picture of measure points

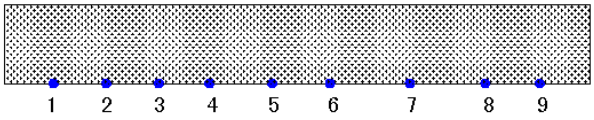

(b) Digram of measure points

Fig. 8 Position of measure points

4.2 Relationship of wave accumulation of floating bridge with velocities and weight of load

It is convinient to compare each case to make x-axis nondemension during analysis dynamic response of floating bridge at same load and various velocities, namely, let vt/L denote x-axis (v is the velocity of load, t is time and L is the length of measure region). Fig. 8 is the temporal vertical displacement variation of the 5th measure point of the floating bridge subjected to load with weight W=16.23N and the x-axis is the nondimensional length vt/L and the y-axis is the vertical displacement (unit is mm) of the measure point of floating bridge. Fig. 8 shows that the amplitude of displacement wave, which is excited by load with velocity of 0.79m/s, is about 1.5mm, as the real line shows. And the accumulations of the displacement wave are about 3.1mm and 2.8mm while the velocities of load are equal to 1.82m/s and 2.96m/s, respectively, just as the dot line and dashed line show (at the nondimension time vt/L=0.3 and vt/L=0.28, respectively). This result infers that the faster is the velocity of load the larger is the wave accumulation. For the wave accumulation with load velocity 1.82m/s is larger than the one with load velocity 2.96m/s, the reason maybe is the influent of water wave or the resonance of floating bridge caused by load with velocity 1.82m/s.

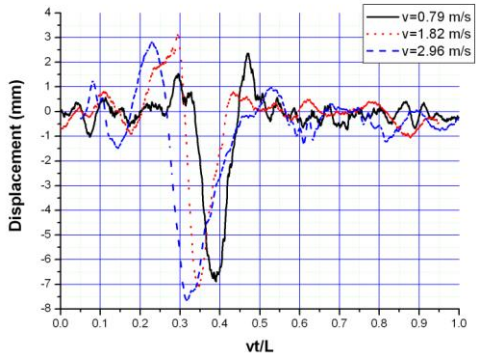

Fig. 8 Temporal displacement variation of the 5th measure point of the floating bridge (W=16.23N)

When the load is heavier, not only the maximum static vertical displacemenis but also the dynamic one are bigger. And the dynamic one is bigger than the static one. Not only is the maximum vertical displacement bigger but also the displace-

ment wave accumulation becomes bigger. Fig. 9 shows the temporal vertical displacement variation of 5th measure point subjected to load with weight W=23.58N. And the displacement wave accumulations are 1.5mm, 5.6mm, and 4.2mm of floating bridge subjected to moving load with velocities of 0.78m/s 1.85m/s and 2.91m/s, respectively.

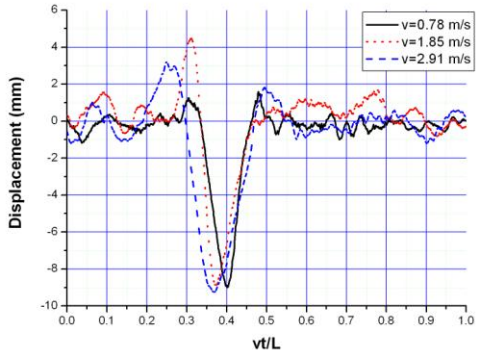

Fig. 9 Temporal displacement variation of the 5th measure point of the floating bridge (W=23.58N)

Fig. 10 shows the temporal vertical displacement variation of 5th measure point subjected to load with weight W=28.49N. And the figure shows that the displacement wave accumulations are 0.2mm, 2.9mm, and 4.8mm of floating bridge subjected to moving load with velocities of 0.78m/s 1.85m/s and 2.91m/s, respectively. As Fig. 8, Fig. 9 and Fig. 10 show, the displacement wave accumulation is related to weight and velocity of the load. And the trend is that faster and heavier is the load, larger is the amplitude of displacement wave, especially the velocity of the load is high. Result will not completely consistent when the velocity of load is low, and this resean maybe concern with the error of experimental measure or brought by influence of random water wave to dynamics of floating bridge.

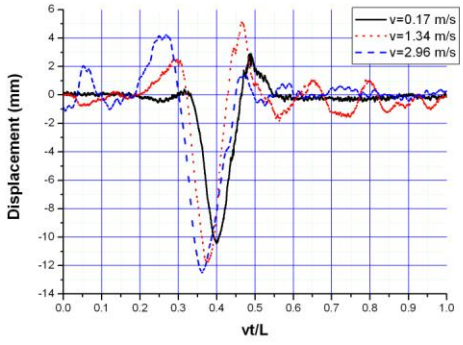

Fig. 10 Temporal displacement variation of the 5th measure point of the floating bridge (W=28.49N)

It is very clear to show the relationship of displacement wave accumulation with the load weight plotting the temporal displacement variation of 5th measure point with same velocity and various weight load. Fig. 11 is temporal vertical displacement variation of floating bridge subjected to load with 0.79m/s. And the figure shows that the maximum displacement wave accumulation is 1.2mm, 1.5mm and 2.3mm under the same velocity and weight equalling to 16.23N, 23.58N and 28.49N, respectively.

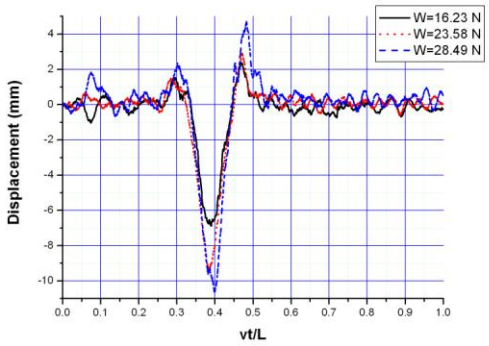

Fig. 11 Temporal displacement variation of 5th measure point of floating bridge with same velocity and different weight (v=0.79m/s)

As Fig. 12 shows, the maximum displacement wave accumulation is 3.1mm, 5.0mm and 5.3mm under the same velocity v=2.91m/s and weight equalling to 16.23N, 23.58N and 28.49N, respectively. The above analyses show that heavier is the load and the more accumulation is the displacement wave. But for the same weight load, the faster is the load, the more accumulation is the displacement wave. And the velocity of load have more effect than the weight of load to accumulation of displacement wave.

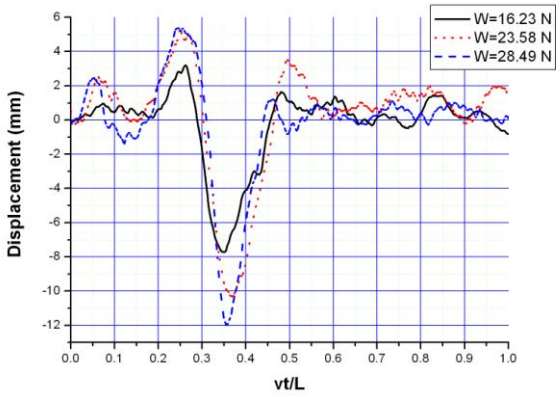

Fig. 12 Temporal displacement variation of 5th measure point of floating bridge with same velocity and different weight (v=2.91m/s)

The displacement wave accumulation can be showed not only from the measure data but also from experimental picture. When the velocity of load equals to v=2.97m/s, the displacement wave accumulation is formed at the frontage of the moving load. And the wave accumulation is larger to shape a "hump", just as the part of the floating bridge within the circle in Fig. 13. The experimental scene shows that the part of the wave accumulation is departed from the water surface and the displacement wave accumulatin is about 5.3mm at this time from the measure data. The displacement wave accumulation is excited by the fast and heavy moving load and propagating

forwards, and the load velocity is equivalent to the one of displacement wave, so the wave accumulation is appeared and the "hump" is shaped.

Fig. 13 Distortion of the floating bridge subjected to fast and heavy moving load

Analysis the experimental kinescope detailedly can be intuitionistic to find that the clear displacement wave accumulation is happened when the load velocity achieves maximum by acceleration. And at this time the displacement wave accumulation in front of load blocks the load to move forwards and make it decelerate. Thus the velocity of load decreases gradually until the displacement wave accumulation is dispeared not to decelerate the load. So at this time the moving load begins to accelerate to gain the maximun velocity, then the displacement wave accumulation and deceleration of load is brought form at a new turn. The above phenomenon is called velocity vibration and the reason for it is that the displacement wave accumulation forming a slope at the floating bridge and the moving load must climb slope to move forwards. And the component of gravity vertical to slope becomes resistance of load moving and it make the load decelerate and this experimental result is consistent to the thoery analysis. The video tape shows that the displacement wave accumulation blocks the load moving with faster velocity.

Another phenomenon after analyzing the video tape is that the moving load undergoes three phases, namely acceleration at the front, no speedup at the middle and deceleration at the back. There is no clear displacement wave accumulation when the moving load is accelerating or decelerating. The distinct displacement wave accumulation is taken place when the moving load is fast, and this means that the displacement wave accumulation is related with the velocity of load not with the acceleration or deceleration of load.

The displacement wave accumulation blocks the load to move forwards and the faster is the load velocity the bigger is the wave accumulation. The structural wave accumulation of floating bridge subjected to fast and heavy load is formed. But there is no water wave accumulation in front of the moving load at the experiment. This means that the structural wave accumulation have more influence and is more direct than the water wave accumulation. Not only the coupled motion of floating bridge and water but also the structural wave accumulation of floating bridge must be included and considered in the pratical engineering.

4 Conclusion

After numerical modeling for floating bridge, numerical computation and analyzing the experimental data, the conclusions are presented as following:

The distinct displacement wave accumulation is formed when the floating bridge is subjected to fast and heavy moving load. And faster and heavier the load is the bigger the displacement wave accumulation is. The accumulation of the displacement wave enlarges resistence of the moving load and it will block the load to move with faster velocity. Because of the accumulation of the displacement wave, the moving load will be presented alternant phases of acceleration and deceleration, namely velocity vibration, with the same power motor.

The structural displacement wave accumulation is more remarkable than the water wave accumulation under the action of fast and heavy load. The displacement wave accumulation of floating bridge and the velocity vibration of moving load exist at the long flexible floating bridge subjected to fast and heavy loads. The problem bringing by the moving loads with heavier weight and higher velocity will possibly come into being at the civil distributing supported and flexible super-long bridges (such as the suspension bridge and the cable-stayed bridge) besides the long flexible floating bridge, which is confronted with the trend of supporting heavier and speedier moving loads and with more flexible structure. There is significant academic value and widely engineering application to study and solve displacement wave accumulation of floating bridge and velocity vibration of moving load.

Acknowledgment

The authors gratefully acknowledge the financial support provided by the National Natural Science Foundation of China (Grant No. 51009147).

References

[1] Timoshenko S. Vibration problem in engineering: 3rd Edition[M], D. van Nostrand Company Inc., 1955.

[2] Y. Sato, S. Okamoto, C. Tamura, et al. Analyses on accumulation of propagating ground surface wave under running train. Wave Propagation, Moving Load and Vibration Reduction: Proceedings of the International Workshop Wave, 2002: 39-46.

[3] Bian Xue-cheng. Ground vibration due to moving load at critical velocity. Journal of Zhejiang University(Engineering Science), 2006, 40(4): 673-675. (in Chinese)

[4] Torbjorn Ekevid, Martin, X. D. Li, Nils-Erik Wiberg. Adaptive FEA of wave propagation induced by high-speed trains. Computers and Structure, 2001, 79: 2693-2704.

[5] Torbjorn Ekevid, Nils-Erik Wiberg. Wave propagation related to high-speed train A scaled boundary FE-approach for unbounded domains. Comput. Methods Appl. Mech. Engrg. 2002, 191: 3947-3964.

[6] Torbjorn Ekevid, Ha kan Lane, Nils-Erik Wiberg. Adaptive solid wave propagation–influences of boundary conditions in high-speed train applications. Comput. Methods Appl. Mech. Engrg. 2006, 195: 236-250.

[7] Y.B. Yang, H.H. Hung, D.W. Chang. Train-induced wave propagation in layered soils using finite/infinite element simulation. Soil Dynamics and Earthquake Engineering, 2003, 23: 263–278.

[8] Chen, YJ, Ju, SH, Ni, SH, and Shen, YJ. Prediction methodology for ground vibration induced by passing trains on bridge structures, J. Sound Vib., 2007, 302(4-5): 806-820.

[9] G Kouroussis, O Verlinden, C Conti. Ground propagation of vibrations from railway vehicles using a finite/infinite-element model of the soil. Journal of Rail and Rapid Transit. 2009, 223(4):405-413.

[10] Yit-Jin Chen, Shiu-Shin Lin, Yi-Jiun Shen. Analysis Model of Ground Vibration Propagation for High-Speed Trains. Geo-Frontiers. 2011, ASCE: 3748-3755.

[11] Y. B. Yang, H. H. Hung, & J. C. Kao. 2.5D FINITE/INFINITE ELEMENT APPROACH FOR SIMULATING TRAIN-INDUCED GROUND VIBRATIONS. AIP Conf. Proc.. 2009, 1233: 5-14.

[12] T.J.R. Hughes, A. Reali, G. Sangalli. Duality and unified analysis of discrete approximations in structural dynamics and wave propagation: Comparison of p-method finite elements with k-method NURBS. Comput. Methods Appl. Mech. Engrg. 2008,197: 4104–4124.

[13] Erkan Çelebi, Seyhan Firat, Günay Beyhan, et al. Field experiments on wave propagation and vibration isolation by using wave barriers. Soil Dynamics and Earthquake Engineering. 2009, 29(5): 824–833.

[14] WANG Cong , FU Shi-xiao , LI Ning, CUI Wei-cheng ,LIN Zhu-ming. Dynamic Analysis of A Pontoon-Separated Floating Bridge Subjected to A Moving Load. China Ocean Engineering. 2006, 20(3): 419-430.

[15] Jong-Shyong WU, Po-Yun Shih. Moving-load-induced Vibrations of a moored floating bridge. Computers & Structures, 1998, 66(4): 435-461.

[16] FU Shi-xiao. Nonlinear hydroelastic analysis of flexible moored structures and floating bridges[D]. Shanghai: Shanghai Jiao Tong university, 2005. (in Chinese)

[17] JIANG Zhao-bing. The Displacement Wave Accumulation Effect of the Long Floating Bridge Multibody System Subjected to Fast and Heavy Loads. Nanjing: The Doctor Thesis of Engineering Institute of Engineering Corps, PLA Univ. of Sci. & Tech, 2008. (in Chinese)